

# Redox Mediation and Photomechanical Oscillations Involving Photosensitive Cyclometalated Ru(II) Complexes, Glucose Oxidase, and Peroxidase

Alexander D. Ryabov,<sup>\*,†</sup> Viktoria S. Kurova,<sup>‡</sup> Ekaterina V. Ivanova,<sup>‡</sup> Ronan Le Lagadec,<sup>§</sup> and Larissa Alexandrova<sup>||</sup>

Department of Chemistry, Carnegie Mellon University, 4400 Fifth Avenue, Pittsburgh, Pennsylvania 15213, Department of Chemistry, Moscow State University, 119899, Moscow, Russia, and Instituto de Química and Instituto de Investigaciones en Materiales, UNAM, Circuito Exterior s/n, Ciudad Universitaria, Mexico, D.F., 04510

Intact photosensitive cyclometalated Ru<sup>II</sup> derivatives of 2-phenylpyridine or *N,N*-dimethylbenzylamine *cis*-[Ru-(C~N)(LL)X<sub>2</sub>]<sub>2</sub>PF<sub>6</sub> [C~N = *o*-C<sub>6</sub>H<sub>4</sub>-py or *o*-C<sub>6</sub>H<sub>4</sub>CH<sub>2</sub>NMe<sub>2</sub>; LL = 1,10-phenanthroline (phen), 2,2'-bipyridine (bpy), or 4,4'-Me<sub>2</sub>-2,2'-bipyridine (Me<sub>2</sub>bpy); X = MeCN or pyridine (py)] are efficient mediators of glucose oxidase (GO) from *Aspergillus niger* and horseradish peroxidase (HRP). Their redox potentials in an aqueous buffer are in the range 0.15–0.35 V versus SCE, and the rate constants for the oxidation GO(red) (where red indicates reduced) by the electrochemically generated Ru<sup>III</sup> species equal  $(1.7\text{--}2.5) \times 10^6 \text{ M}^{-1} \text{ s}^{-1}$  at pH 7 and 25 °C. The redox potentials of all complexes decrease cathodically by 0.4–0.6 V upon irradiation by visible light because of the photoinduced solvolysis of acetonitrile or py ligands. These in situ generated species display an even better mediating performance with HRP, although their behavior toward GO is different. The loading of a ruthenium unit into the protein interior brings about large catalytic currents in a self-assembled system GO–Ru–D-glucose. The estimated rate constant for intramolecular electron transfer from FADH<sub>2</sub> of the active site at Ru<sup>III</sup>,  $k_{\text{intra}}$ , equals  $4.4 \times 10^3 \text{ s}^{-1}$ . This suggests that the distance between the redox partners is around 19 Å. The value of 21 Å was obtained through the docking analysis of a possible closest-to-FAD localization of a Ru-containing fragment derived from the irradiated complex *cis*-[Ru(*o*-C<sub>6</sub>H<sub>4</sub>-py)(phen)(MeCN)<sub>2</sub>]<sub>2</sub>PF<sub>6</sub>. The operational stability of the GO–Ru assemblies depends on the nature of complex used, the highest being observed for *cis*-[Ru(*o*-C<sub>6</sub>H<sub>4</sub>-py)(Me<sub>2</sub>bpy)(MeCN)<sub>2</sub>]<sub>2</sub>PF<sub>6</sub> (2). UV–vis studies of interaction of 2 with GO revealed photomechanical oscillations in the system GO–Ru–D-glucose. When irradiated complex 2 is mixed with GO and D-glucose, the absorbance at 510 nm increases because of the enzymatic reduction of Ru<sup>III</sup> to Ru<sup>II</sup>. The absorbance drops rapidly and then increases as in the first cycle after shaking the reaction solution. Many cycles are possible, and the rate of absorbance

increase does not depend on a cycle number. A plausible mechanism of the oscillations is presented.

Transition metal complexes are among the best-known materials for moving electrons between active sites of redox enzymes and electrodes.<sup>1</sup> The metal ion is the key unit, surrounded by a set of ligands that bring about features essential for fast exchange of electrons at the lowest applied potential.<sup>2–6</sup> Referred to as electron shuttles or mediators, such molecules should generally have a medium-resistant, invariable redox potential. The coordination sphere of the transition metal should be intolerant to ligand substitution; otherwise, its redox potential might be affected. In contrast, if a mediator rapidly changes its redox characteristics, for example, upon irradiation, this new feature is advantageous for designing photosensitive bioamperometric analytical devices.<sup>7,8</sup> Irradiation alters the redox potential of a transition metal mediator if it contains photosensitive ligands. Previously, we reported on the substitutionally inert cyclometalated mediators [Ru<sup>II</sup>(*o*-C<sub>6</sub>H<sub>4</sub>-X)(LL)<sub>2</sub>]<sub>2</sub>PF<sub>6</sub> (X = 2-pyridinyl, 2-imidazolyl, or CH<sub>2</sub>NMe<sub>2</sub>; LL = bpy or phen) that are involved in the fast electron exchange with horseradish peroxidase (HRP), peroxidases from other sources, and glucose oxidase (GO).<sup>9–11</sup> The corresponding rate constants usually equal  $10^7\text{--}10^8 \text{ M}^{-1} \text{ s}^{-1}$ , whereas their nontunable redox

\* Corresponding author. E-mail: ryabov@andrew.cmu.edu. Fax: (412) 268-1061.

† Carnegie Mellon University.

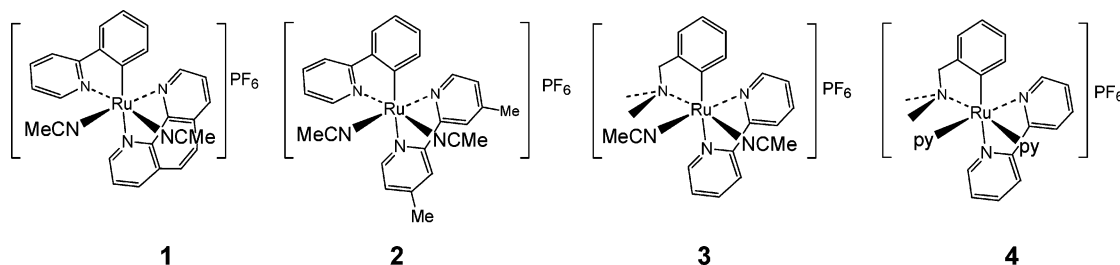
‡ Moscow State University.

§ Instituto de Química, Ciudad Universitaria.

|| Instituto de Investigaciones en Materiales, Ciudad Universitaria.

- (1) Ryabov, A. D. *Adv. Inorg. Chem.* **2004**, *55*, 201–270.
- (2) Turner, A. P. F.; Karube, I.; Wilson, G. S. *Biosensors. Fundamentals and Applications*; Oxford University Press: Oxford, U.K., 1987.
- (3) Wilson, R.; Turner, A. P. F. *Biosens. Bioelectron.* **1992**, *7*, 165–185.
- (4) Willner, I.; Willner, B. *Trends Biotechnol.* **2001**, *19*, 222–230.
- (5) O'Connell, P. J.; Guilbault, G. G. *Anal. Lett.* **2001**, *34*, 1063–1078.
- (6) Castillo, J.; Gáspár, S.; Leth, S.; Niculescu, M.; Mortari, A.; Bontidean, I.; Soukharev, V.; Dorneanu, S. A.; Ryabov, A. D.; Csörgi, E. *Sens. Actuators B: Chem.* **2004**, *102*, 179–194.
- (7) Willner, I.; Willner, B. *Bioelectrochem. Bioenerg.* **1997**, *42*, 43–57.
- (8) Willner, I.; Katz, E. *Angew. Chem., Int. Ed.* **2000**, *39*, 1180–1218.
- (9) Ryabov, A. D.; Soukharev, V. S.; Alexandrova, L.; Le Lagadec, R.; Pfeffer, M. *Inorg. Chem.* **2001**, *30*, 6529–6532.
- (10) Soukharev, V. S.; Ryabov, A. D.; Csörgi, E. *J. Organomet. Chem.* **2003**, *668*, 75–81.

## Chart 1. Cyclometalated Photosensitive Ruthena(II)Cycles Used in This Study



potentials are in the range 150–300 mV versus SCE. In our subsequent publication, we described the synthesis of and characterized new *phototunable* cyclometalated Ru<sup>II</sup> complexes of 2-phenylpyridine or 2-(4-tolyl)pyridine *cis*-[Ru<sup>II</sup>(*o*-C<sub>6</sub>H<sub>4</sub>-X)(LL)-(MeCN)<sub>2</sub>]PF<sub>6</sub> or *cis*-[Ru<sup>II</sup>(*o*-C<sub>6</sub>H<sub>4</sub>-X)(LL)(py)<sub>2</sub>]PF<sub>6</sub> (**1–4**) with *cis* acetonitrile or pyridine ligands. Their redox potentials are reduced by 0.3–0.8 V in minutes when their solutions in MeOH are irradiated by visible light.<sup>12</sup> This work deals with studies of mediating properties of these complexes, both intact and irradiated, with respect to GO from *Aspergillus niger* and HRP. It has been demonstrated that intact compounds **1–4** shown in Chart 1 are good mediators for both enzymes. When irradiated in buffered aqueous solutions, the mediators function well with HRP at significantly lower potentials. Unique catalytic currents are observed in the irradiated system **1**–GO–D-glucose because of a loading of an aqua derivative of **1** onto a GO globule. This effect is analyzed in some detail using a computer simulation of electrochemical data and a docking analysis of possible binding sites of aquated complex **1** and the GO enzyme. New photo-mechanical oscillations in the system **2**–GO–D-glucose are also described.

### EXPERIMENTAL SECTION

**Materials.** Ruthenium complexes **1**, **3**, and **4** were prepared as described in our previous publications;<sup>9,12,13</sup> the synthesis of **2** is detailed below. D-(+)-Glucose (0.45 g; anhydrous, ICN Biomedicals, or monohydrate, Fluka) was dissolved in 2.5 mL of 0.01 M phosphate buffer (pH 7.0) to give a 1 M solution that was kept overnight for equilibration between the  $\alpha$  and  $\beta$  anomers. Glucose oxidase (0.02 g) from *A. niger* (EC 1.1.3.4, Sigma, type X-S, 200 U mg<sup>-1</sup>; ICN Biomedicals 250 U mg<sup>-1</sup>) was dissolved in 0.1 mL of 0.01 M phosphate buffer (pH 7.0), and the concentration of active FAD was determined spectrophotometrically by measuring the decrease in absorbance at 450 nm ( $\epsilon_{450} = 1.31 \times 10^4 \text{ M}^{-1} \text{ cm}^{-1}$ ) after addition of 0.05 M D-glucose.<sup>14</sup> The frozen solution was stored at –18 °C. HRP (5 mg, Sigma) was dissolved in 2 mL of distilled water and kept frozen at –18 °C.

**Synthesis of Complex 2.** Complex [Ru(*o*-C<sub>6</sub>H<sub>4</sub>-py)(MeCN)<sub>4</sub>]-PF<sub>6</sub><sup>15</sup> (0.50 g, 0.886 mmol) and 4,4'-dimethyl-2,2'-dipyridine (0.163

g, 0.891 mmol) were degassed in a vacuum, the flask was purged three times with N<sub>2</sub>, and dry MeCN (70 mL) was then added. The mixture was stirred at 40 °C under nitrogen for 48 h to afford a dark-brown solution. The solvent was evaporated; the residue was dissolved in 10 mL of CH<sub>2</sub>Cl<sub>2</sub> and brought on a column with basic Al<sub>2</sub>O<sub>3</sub>. The product was eluted with 1.5% MeCN in CH<sub>2</sub>Cl<sub>2</sub>. The first band was collected, concentrated, poured into ether, and kept in a freezer. Brown crystals of **2** (0.170 g, 29%) were separated and dried in the air. IR: 842 (vs, PF<sub>6</sub>), 2263 (m, MeCN). Anal. Found: C, 43.72; H, 3.75; N, 8.40. Calcd for C<sub>27</sub>H<sub>26</sub>F<sub>6</sub>N<sub>5</sub>Ru·1.5CH<sub>2</sub>Cl<sub>2</sub>: C, 43.72; H, 3.75; N, 8.40%.

**Methods.** Photolysis of Ru<sup>II</sup> complexes **1–4** was carried out either with a WKO ENX 360 W lamp as described previously<sup>12</sup> or with a conventional halogen lamp in 10–40 min at room temperature. The reaction progress was monitored by cyclic voltammetry at a scan rate 50 mV s<sup>-1</sup> in the potential range from –0.40 to 0.70 V (SCE). Electronic spectra were obtained on a Shimadzu U-160A spectrophotometer. Electrochemical measurements were performed on a PC-interfaced potentiostat–galvanostat IPC-2 with the IPC-4 software package (Institute of Physical Chemistry, RAS, Moscow, Russia) or an EG&G Princeton Applied Research 263A instrument. A three-electrode setup was used with a BAS working glassy carbon electrode, saturated calomel or Ag/AgCl reference electrodes, and auxiliary Pt electrode. Before measurements, the working electrode was polished with a diamond paste and rinsed with ethanol and distilled water. Anodic peak currents (*i*<sub>o</sub>) were obtained from cyclic voltammograms in the absence of the enzyme. Catalytic currents (*i*<sub>cat</sub>) were obtained in the presence of GO and D-glucose. The rate constants, *k*<sub>et</sub>, were calculated from the slopes of linear plots of the ratio *i*<sub>cat</sub>/*i*<sub>o</sub> against ([GO]/*v*)<sup>1/2</sup> (*v* is the scan rate), as originally described elsewhere<sup>16</sup> and applied in our previous studies.<sup>9,10,17,18</sup>

**Computer Simulations: (A) Docking.** Theoretical calculations of the geometrical correspondence between the structures of GO and complex **1** were performed using a docking method based on the GRAMM package.<sup>19,20</sup> The X-ray crystallographic data for GO obtained at 2.3-Å resolution<sup>21</sup> was used to acquire

- (11) Alpeeva, I. S.; Soukharev, V. S.; Alexandrova, L.; Shilova, N. V.; Bovin, N. V.; Csöregi, E.; Ryabov, A. D.; Sakharov, I. Y. *J. Biol. Inorg. Chem.* **2003**, *8*, 683–688.
- (12) Ryabov, A. D.; Le Lagadec, R.; Estevez, H.; Hernandez, S.; Alexandrova, L.; Kurova, V. S.; Fischer, A.; Pfeffer, M. *Inorg. Chem.*, manuscript submitted.
- (13) Le Lagadec, R.; Rubio, L.; Alexandrova, L.; Toscano, R. A.; Ivanova, E. V.; Meškys, R.; Laurinavicius, V.; Pfeffer, M.; Ryabov, A. D. *J. Organomet. Chem.* **2004**, *689*, 4820–4932.
- (14) Weibel, M. K.; Bright, H. J. *J. Biol. Chem.* **1971**, *246*, 2734–2744.
- (15) Fernandez, S.; Pfeffer, M.; Ritleng, V.; Sirlin, C. *Organometallics* **1999**, *18*, 2390–2394.

- (16) Bourdillon, C.; Demaille, C.; Moiroux, J.; Savéant, J.-M. *J. Am. Chem. Soc.* **1993**, *115*, 2–10.
- (17) Ryabov, A. D.; Firsova, Y. N.; Goral, V. N.; Ryabova, E. S.; Shevelkova, A. N.; Troitskaya, L. L.; Demeschik, T. V.; Sokolov, V. I. *Chem. Eur. J.* **1998**, *4*, 806–813.
- (18) Ryabov, A. D.; Soukharev, V. S.; Alexandrova, L.; Le Lagadec, R.; Pfeffer, M. *Inorg. Chem.* **2003**, *42*, 6598–6600.
- (19) Katchalski-Katzir, E.; Shariv, I.; Eisenstein, M.; Friesem, A. A.; Aflalo, C.; Vakser, I. A. *Proc. Natl. Acad. Sci. U.S.A.* **1992**, *89*, 2195–2199.
- (20) Vakser, I. A.; Matar, O. G.; Lam, C. F. *Proc. Natl. Acad. Sci. U.S.A.* **1999**, *96*, 8477–8482.
- (21) Hecht, H. J.; Kalisz, H. M.; Hendle, J.; Schmid, R. D.; Schomburg, D. *J. Mol. Biol.* **1993**, *229*, 153–172.

**Table 1. Redox Potentials and Spectral Properties of Intact and Irradiated Complexes 1–4 and Rate Constants for the Oxidation of Reduced D-Glucose GO from *A. niger* by Electrochemically Generated Intact Ru<sup>III</sup> Species at pH 7 (0.1 M Phosphate, 5% MeOH) and 25 °C**

complex	$E_{1/2}/V$ versus SCE		$k_{et}/M^{-1} s^{-1}$	$\lambda_{max}/nm$	
	intact	irradiated		intact	irradiated
1	0.35 (0.54) <sup>a</sup>	-0.25 ± 0.01	$(1.7 \pm 0.1) \times 10^6$	396, 466	384, 533
2	0.33 (0.52) <sup>a</sup>	-0.28 ± 0.01	$(2.5 \pm 0.1) \times 10^6$	383, 464	346, 534
3	0.30 (0.50) <sup>a</sup>	-0.17 ± 0.01	$(2.0 \pm 0.1) \times 10^6$	369, 462	349, 541
4	0.15 (0.30) <sup>a</sup>	-0.17 ± 0.01	$(1.8 \pm 0.1) \times 10^6$	470	542

<sup>a</sup> In MeOH as solvent.

the geometric parameters of the enzyme. The corresponding information for complex 1 is presented elsewhere.<sup>22</sup>

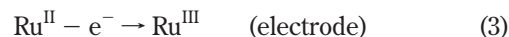
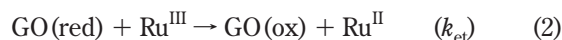
**(B) Cyclic Voltammetry.** Simulation of the cyclic voltammograms was performed using the CVSIM software package.<sup>23</sup> The adopted mechanism is shown in Scheme 1. The rate constant for the heterogeneous electron transfer  $k_{het} = 0.01 \text{ cm s}^{-1}$  was used. It corresponds to a quasireversible process. The  $\alpha$  parameter was 0.5, the diffusion coefficient for GO was taken as  $4.1 \times 10^{-7} \text{ cm}^2 \text{ s}^{-1}$ ,<sup>24,25</sup> the surface area of the working electrode was  $0.071 \text{ cm}^2$ , and the scan rate was  $5 \text{ mV s}^{-1}$  at 25 °C.

**Photomechanical Oscillations.** A methanol solution of complex 2 was irradiated with a halogen lamp for 10 min. Then an aliquot was added to a buffered aqueous solution (0.05 M phosphate, pH 7), followed of D-glucose and GO. The final concentrations of complex 2, D-glucose, and GO in the UV-vis cell were  $1 \times 10^{-4}$ , 0.03, and  $1 \times 10^{-7} \text{ M}$ , respectively. The cell was removed from the cell compartment when the absorbance reached a constant value at 510 nm and was then shaken vigorously. Rapid fading was observed. The cell was returned to the cell compartment, and the absorbance change was registered again. This procedure was repeated several times.

## RESULTS AND DISCUSSION

**Mediating Performance of Intact Ruthena(II)cycles with Glucose Oxidase.** Studies by cyclic voltammetry of intact ruthena(II)cycles 1–4 in buffered aqueous solution showed an almost Nernstian behavior at the glassy carbon electrode at scan rates of 2–100  $\text{mV s}^{-1}$ . An insignificant complication encountered for complex 2 was adsorption on the electrode surface,<sup>26</sup> which was manifested as a ca. 30% increase in anodic peak current during the second scan at a scan rate  $50 \text{ mV s}^{-1}$ . As has been previously observed for substitutionally inert ruthena(II)cycles,<sup>9</sup> catalytic currents increase noticeably upon addition of D-glucose to solutions of 1–4 and GO, indicating that the electrochemically generated Ru<sup>III</sup> species rapidly oxidize the reduced active site of GO (step 2 in the mechanism of bioelectrocatalysis mediated by glucose oxidase is represented by reactions 1–3, where stoichiometric coefficients are omitted for clarity and red and ox indicate

reduced and oxidized, respectively). The corresponding second-order rate constants,  $k_{et}$ , calculated according to the procedure of Bourdillon et al.<sup>16</sup> are summarized in Table 1. The rate constants,  $k_{et}$ , for the most active transition metal mediators of GO from *A. niger* are slightly higher than  $10^7 \text{ M}^{-1} \text{ s}^{-1}$ . The data in Table 1 show that the reactivities of complexes 1–4 are slightly lower than the highest known reactivity.



All four complexes studied display similar reactivities toward GO(red). The insignificant variation of their redox potentials does not affect  $k_{et}$ , as expected.<sup>1</sup> The nature of the cyclometalated ligand, viz., 2-phenylpyridine or *N,N*-dimethylbenzylamine, has a minor influence on  $k_{et}$ . The values of  $k_{et}$  for metalacycles 1–4 are at least 1 order of magnitude higher than those for a series of acido ruthenium(II/III) complexes without cyclometalated ligand.<sup>27</sup>

**Photochemical Properties of Ruthena(II)cycles in Buffered Aqueous Solution.** We previously demonstrated that irradiating cyclometalated Ru<sup>II</sup> complexes with cis MeCN ligands in methanol creates new species with significantly, up to 0.8 V, lower redox potentials as a result of photoinduced solvolysis of the nitrile ligands.<sup>12</sup> The low-potential mediators thus formed are particularly interesting, and therefore, it has been challenging to investigate their performance with “signature” enzymes such as GO and HRP.<sup>1</sup> This was preceded by studies of the photochemical properties of complexes 1–4 in buffered aqueous solution.

The “dark” cyclic voltammogram of 1 at pH 7 is represented by the solid line in Figure 1. There is one well-defined feature around 0.5 V in the potential range from -0.5 to 1 V because of a Ru<sup>II/III</sup> event. When the solution is irradiated, the 0.5 V peak disappears in a matter of few minutes, and the new cyclic voltammogram given by the dashed line in Figure 1, which does not change upon further irradiation, is obtained. A peak at around 0.0 V replaces the 0.5 V peak. An overall potential decrease is 0.5 V. This behavior is analogous to the electrochemical behavior of 1 in MeOH and can be rationalized in terms of the photosubstitution of the strong  $\pi$ -acceptor acetonitrile ligands by components

(22) Ryabov, A. D.; Kurova, V. S.; Alexandrova, L.; Le Lagadec, R.; Pfeffer, M., Supporting Information to ref 12.

(23) Gosser, D. K., Jr. *Cyclic Voltammetry. Simulation and Analysis of Reaction Mechanisms*; VCH: Weinheim, Germany, 1993.

(24) Nakamura, S.; Hayashi, S.; Koga, K. *Biochim. Biophys. Acta* **1976**, *445*, 294–308.

(25) Degani, Y.; Heller, A. *J. Am. Chem. Soc.* **1988**, *110*, 2615–2620.

(26) Bond, A. M. *Modern Polarographic Methods in Analytical Chemistry*; Marcell Dekker: New York, 1980.

(27) Kurova, V. S.; Ershov, A. Y.; Ryabov, A. D. *Izv. RAN, Ser. Khim.* **2001**, *50*, 1766–1771.

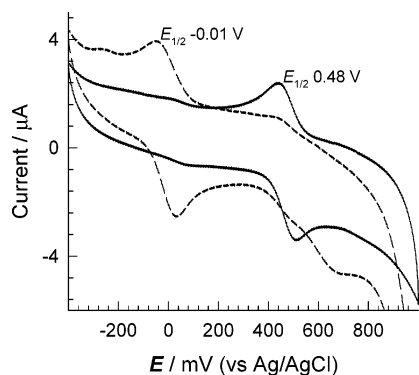
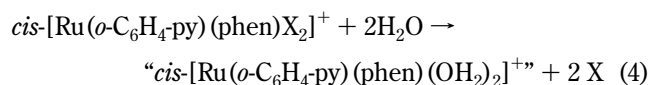


**Figure 1.** Cyclic voltammograms of intact complex **1** (solid line) and the product of its photosolvolysis (dashed line) at pH 7 and 22 °C. Conditions:  $[1] = 3.3 \times 10^{-4}$  M,  $[\text{phosphate}] = 0.01$  M,  $[\text{Triton X-100}] = 2\%$ , scan rate =  $0.2 \text{ V s}^{-1}$ , irradiation time (360-W lamp) = 4 min.

of the buffered solution such as water (eq 4).<sup>12</sup>

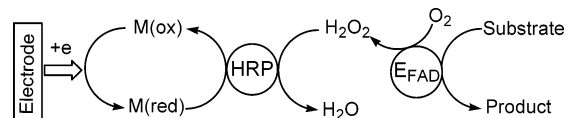


The data shown in Figure 1 were obtained in the presence of the neutral surfactant Triton X-100, which is known to increase observed redox potentials of transition metal complexes.<sup>28</sup> The surfactant is added to stabilize the solutions and prevent the precipitation of complexes **1–4** due to their limited solubility at pH 7. Adding an organic cosolvent such as MeOH also increases the solubility. The data obtained in the presence of 5% (v/v) MeOH in the absence of Triton X-100 are reported in Table 1. The minor variation of the medium composition does not change the nature of the photochemical process: the redox potentials of all complexes studied underwent fairly marked cathodic shifts.

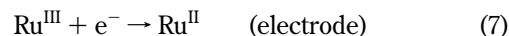
Photosolvolysis affects the electronic spectra of complexes **1–4**. The intact complexes have absorption bands at 370–410 and 460–470 nm at pH 7. Irradiation induces a 20–40-nm blue shift of the former band but caused the band at 460–480 nm to disappear. These changes are followed by much slower secondary process, which manifests itself in an absorbance growth at 530–560 nm and lasts for several hours. The second phase is presumably because of an interaction of the intermediate formed via eq 4 with dioxygen to afford either the corresponding Ru<sup>III</sup> complex or dinuclear  $\mu$ -oxo species similar to those reported elsewhere.<sup>12,29</sup>

**Mediating Performance of Intact and Irradiated Ruthena-(II)cycles with Horseradish Peroxidase.** Reduction of the oxidized forms of HRP, i.e., its compounds I and II,<sup>30</sup> by a low-molecular-weight transition metal mediator is a key feature in the functioning of modern amperometric biosensors.<sup>6</sup> The reason is that H<sub>2</sub>O<sub>2</sub> produced by the reported redox enzymes, usually FAD-dependent oxidases, is detected in the HRP catalytic cycle (Scheme 1).<sup>1</sup> The potential of the working electrode should be

### Scheme 1. Principle of Action of a Bienzyme Biosensor Incorporating HRP, an FAD-dependent Oxidase (E<sub>FAD</sub>), and an Electron Shuttle



set as low as possible to avoid background oxidation of interfering substances.<sup>6</sup> Therefore, complexes **1–4** are, in fact, promising. Depending on the particular task, they are capable of mediating electron exchange at significantly different redox potentials: the potential ranges for the intact and irradiated compounds are 0.15–0.35 and (–0.35)–(–0.15) V (versus SCE), respectively. Both forms, i.e., intact and irradiated, reduce the oxidized states of HRP, i.e., compounds I and II, and the irradiation is performed in a matter of minutes. This is exemplified by using intact and irradiated complex **1** in the mediated HRP-catalyzed bioelectroreduction of H<sub>2</sub>O<sub>2</sub>. Hydrogen peroxide does not affect cyclic voltammograms of intact complex **1**. However, the cathodic current increases sharply in the presence of HRP (Figure 2A), in accordance with the following catalytic cycle:<sup>31–33</sup>



Here, HRP-I/II represents HRP compound I or II. The cathodic current increases with increasing concentration of H<sub>2</sub>O<sub>2</sub>. Figure 2B illustrates the system when complex **1** has been irradiated before addition of H<sub>2</sub>O<sub>2</sub> and HRP. The data indicate that the irradiated complex does reduce compounds I and II. The currents in the irradiated system B are higher than those in system A at the same H<sub>2</sub>O<sub>2</sub> concentration because of the higher driving force of reaction 6: the redox potential of the mediator decreases by 0.45 V, whereas its size is unaffected.<sup>34</sup> To this end, the same Ru-based mediators with photochemically controlled redox potentials provide species that can function at different potentials of a working electrode. Noteworthy is the fact that the potential of the irradiated Ru mediator does not change during the electrocatalysis with HRP, suggesting the absence of binding between the ruthenium complex and the HRP protein. As shown below, this is not the case for the GO enzyme, which traps and binds ruthenium species during electrocatalysis.

**Mediating Performance of Irradiated Ruthena(II)cycles with Glucose Oxidase.** The electrochemical behaviors of irradiated complexes **1–4** toward HRP and FAD-dependent GO from *Aspergillus niger* are different. Cyclic voltammogram of irradiated **1** in the presence of GO is shown in Figure 3a. In contrast to intact complexes **1–4** (see above), addition of D-glucose gives

(31) Gorton, L. *Electroanalysis* **1995**, *7*, 23–44.

(32) Gorton, L.; Lindgren, A.; Larsson, T.; Munteanu, F. D.; Ruzgas, T.; Gazaryan, I. *Anal. Chim. Acta* **1999**, *400*, 91–108.

(33) Dequaire, M.; Limoges, B.; Moiroux, J.; Saveant, J.-M. *J. Am. Chem. Soc.* **2002**, *124*, 240–253.

(34) Ryabov, A. D.; Goral, V. N.; Ivanova, E. V.; Reshetova, M. D.; Hradsky, A.; Bildstein, B. *J. Organomet. Chem.* **1999**, *589*, 85–91.

(28) Ryabov, A. D.; Amon, A.; Gorbatova, R. K.; Ryabova, E. S.; Gnedenko, B. B. *J. Phys. Chem.* **1995**, *99*, 14072–14077.

(29) Schoonover, J. R.; Ni, J.-F.; Roecker, L.; White, P. S.; Meyer, T. J. *Inorg. Chem.* **1996**, *35*, 5885–5892.

(30) Dunford, H. B. *Heme Peroxidases*; Wiley-VCH: New York, 1999.

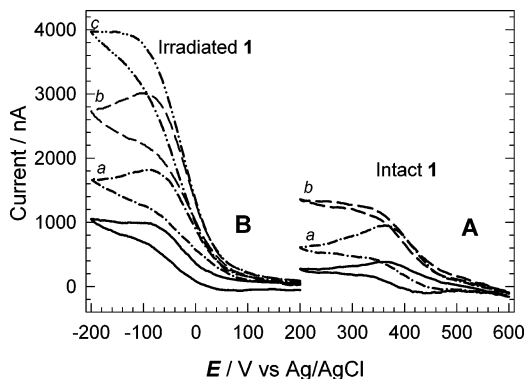


**Figure 2.** Bioelectrocatalysis involving **1** ( $1.2 \times 10^{-4}$  M), HRP ( $6 \times 10^{-6}$  M), and (a) 0.35, (b) 0.7, and (c) 1.05 mM  $\text{H}_2\text{O}_2$  at pH 7, 22 °C, and a scan rate of  $5 \text{ mV s}^{-1}$ : (A) before and (B) after irradiation with a 360-W lamp for 4 min.

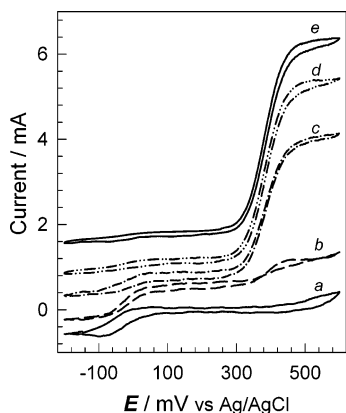


**Figure 3.** Cyclic voltammograms of irradiated complex **1** (a) in the presence  $\text{D-glucose}$  (b) in the presence of GO, (c–e) in the presence of GO right after Spectrum b was recorded. Conditions:  $[\mathbf{1}] = 1.1 \times 10^{-4}$  M,  $[\text{GO}] = 3 \times 10^{-6}$  M,  $[\text{D-glucose}] = 0.05$  M, 20 °C, pH 7, scan rate =  $5 \text{ mV s}^{-1}$ .

rise to a weak catalytic current around 0 V, as the driving force of reaction 2 is low for the fast oxidation of GO(red) by  $\text{Ru}^{\text{III}}$  (Figure 3b). However, a strong catalytic current is observed at higher potentials during sequential scans (Figure 3c–e). The current at 0 V is negligible, whereas that at 0.4 V becomes quite large (Figure 3d,e). The maximum current achieved after four consecutive scans (Figure 3e) does not increase further. The data in Figure 3 indicate two principal effects. First, the ligands at ruthenium change during bioelectrochemical reactions, as suggested by the large variation of the redox potential.<sup>27,35</sup> Second, the change at ruthenium is favorable for the oxidation of GO(red) by electrochemically generated  $\text{Ru}^{\text{III}}$  species. The anodic shift of the potential by  $\sim 0.4$  V supports the conclusion that ruthenium either coordinates an extra ligand such as imidazole<sup>27,35</sup> or becomes trapped somewhere in the protein interior and shielded by hydrophobic amino acid residues of the protein without forming new coordinative bonds.

The maximum catalytic current is a function of the concentration of the ruthenium complex introduced. Studied for complexes **2** and **3** as examples, the current first grows with increasing the concentration of added **2** or **3** and then levels off (Figure 4),

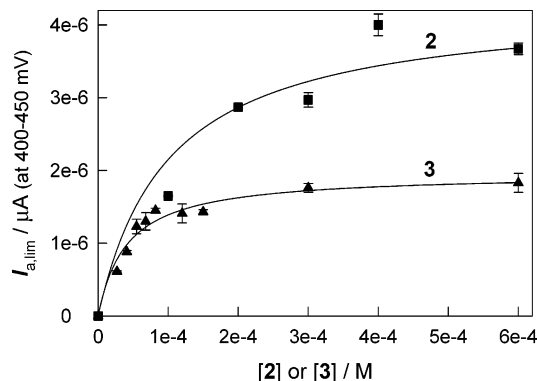


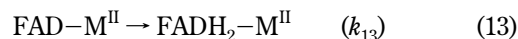
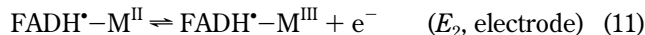
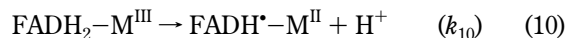
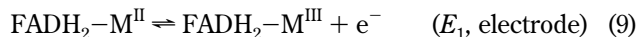
**Figure 4.** Limiting catalytic anodic currents of the second wave (around 0.4–0.5 V) as a function of the concentrations of irradiated complexes ( $\blacksquare$ ) **2** and ( $\blacktriangle$ ) **3** in the presence of GO ( $3 \times 10^{-6}$  M) and  $\text{D-glucose}$  (0.1 M). Conditions: scan rate =  $5 \text{ mV s}^{-1}$ , pH 7 (0.01 M phosphate), 25 °C.

suggesting intramolecular electron transfer. Both dependencies fit the electrochemical version of the Michaelis–Menten equation

$$I_{a,\text{lim}} = \frac{I_{a,\text{lim}}^{\text{max}} [\text{Ru}]_t}{K_S + [\text{Ru}]_t} \quad (8)$$

Here,  $K_S$  refers to the dissociation constant for the electrochemically active “GO–Ru” intermediate, and  $I_{a,\text{lim}}^{\text{max}}$  is the maximum limiting anodic current. The  $K_S$  values obtained by fitting the data in Figure 4 to eq 8 equal  $(1.8 \pm 0.7) \times 10^{-4}$  and  $(0.42 \pm 0.07) \times 10^{-4}$  M, and the  $I_{a,\text{lim}}^{\text{max}}$  values equal  $5.6 \pm 0.2$  and  $1.8 \pm 0.1$  mA for complexes **2** and **3**, respectively, at  $[\text{GO}] = 3 \times 10^{-6}$  M. The difference in performance of **2** and **3** is insignificant, but complex **2** is slightly more active.

**Quantitation of the Efficacy of Intramolecular Electron Transfer within a GO–Ru Assembly.** Assuming that the cyclic voltammogram in Figure 3e reflects intramolecular electron transfer from the reduced flavin adenine dinucleotide ( $\text{FADH}_2$ ) of GO at  $\text{Ru}^{\text{III}}$ , the electrochemical data were simulated to evaluate the corresponding first-order rate constant  $k_{\text{intra}}$ . The analysis was performed in terms of reactions 9–13 as suggested by Badia et al.<sup>36</sup>



Here,  $\text{FADH}_2\text{--M}^{\text{II}}$  is the complex between reduced GO and  $\text{Ru}^{\text{II}}$ , which is oxidized at the electrode to generate the corresponding  $\text{Ru}^{\text{III}}$  species. The subsequent electron transfer (eq 10) gives the semireduced  $\text{FADH}^{\cdot}$  intermediate complexed with  $\text{Ru}^{\text{II}}$ . This is then finally oxidized into FAD (eq 12) after the electrode reaction

(35) Lever, A. B. V. *Inorg. Chem.* **1990**, *29*, 1271–1285.

(36) Badia, A.; Carlini, R.; Fernandez, A.; Battaglini, F.; Mikkelsen, S. R.; English, A. M. *J. Am. Chem. Soc.* **1993**, *115*, 7053–7060.

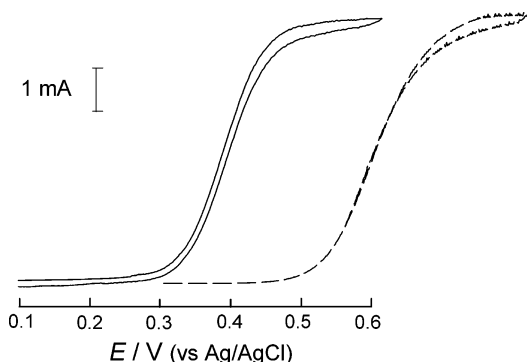


**Figure 5.** Experimental (solid line, left) and simulated (dashed line, right) cyclic voltammograms of irradiated complex **1** in the presence D-glucose and GO. Figure 3e was selected for simulation. The x scale refers to the left cyclic voltammogram. Conditions are as in Figure 3.

11. Reaction 13 is the reduction of FAD by excess of D-glucose;  $i_{\max} = 2FA(D_{\text{GO}}k_{\text{intra}})^{1/2}[\text{GO}-\text{M}]$  and  $k_{\text{intra}} = k_{10}k_{12}/(k_{10}^{1/2} + k_{12}^{1/2})^2$  [ $D_{\text{GO}}$  is the diffusion coefficient for GO,  $F$  is the Faraday constant (96 500 C mol<sup>-1</sup>) and  $A$  is the electrode area (cm<sup>2</sup>)].<sup>36</sup> The rate constant  $k_{\text{intra}}$  was obtained as described elsewhere.<sup>23</sup> A satisfactory match between the experimental and calculated cyclic voltammograms shown in Figure 5 was achieved under the following assumptions:  $k_{10} = k_{12} = 17\,500\text{ s}^{-1}$ ,  $E_1 = E_2$ ,<sup>36</sup>  $k_{13} = 800\text{ s}^{-1}$  (at the saturating glucose concentration),<sup>14</sup>  $D_{\text{GO}} = 4.1 \times 10^{-7}\text{ cm}^2\text{ s}^{-1}$ ,  $\alpha = 0.5$ , and  $k_{\text{het}} = 0.05\text{ cm s}^{-1}$ . The calculated rate constant  $k_{\text{intra}}$  equals 4375 s<sup>-1</sup>. The highest previously reported values of  $k_{\text{intra}}$  were observed upon modification of native GO by [Ru(phen)<sub>2</sub>]<sup>2+</sup> and [Ru(bpy)<sub>2</sub>]<sup>2+</sup> units, viz., 70 and 12 s<sup>-1</sup>, respectively.<sup>37</sup> The value for a reconstituted GO preparation with FAD modified with a ferrocene unit equals 40 s<sup>-1</sup>.<sup>38</sup> The rate constant  $k_{\text{intra}}$  found in this work is significantly larger, suggesting a favorable localization of the mediator within the GO enzyme. It has been argued that  $k_{\text{intra}}$  values in proteins are largely determined by the distance between the redox partners.<sup>39</sup> Here, the partners are the lumichrome of FAD and the Ru complex. The edge-to-edge distance between the two centers can be approximated from  $k_{\text{intra}}$ .<sup>39</sup> The value of 4375 s<sup>-1</sup> suggests an 18.9-Å separation. As shown below, a theoretical simulation of the closest approach of Ru to FAD gives a comparable separation.

**Docking Simulation of Possible Localization of the Ru Fragment within a Protein (GO) Globule.** The X-ray crystallographic data for GO from *A. niger*<sup>21</sup> and complex **1**<sup>12</sup> were used to probe possible geometric sites for the localization of irradiated **1** within the GO globule. The docking routine using the GRAMM software package was applied.<sup>19,20</sup> Because complex **1** loses MeCN upon irradiation, atomic coordinates for **1** without the two MeCN ligands were used, i.e., it was assumed that the four-coordinated ruthenium moiety “[Ru(*o*-C<sub>6</sub>H<sub>4</sub>-py)(phen)]” is involved. This assumption is justified because, if *cis*-[Ru(*o*-C<sub>6</sub>H<sub>4</sub>-py)(phen)(OH<sub>2</sub>)<sub>2</sub>]<sup>n+</sup> were to react with GO, the aqua ligands might be substituted by donor amino acid residues of the protein. Aqua ligands at ruthenium could belong to the protein, i.e., be water molecules

that are an integral part of the protein structure. Several protein sites were localized, the geometries of which correspond to the thus-designed ruthenium fragment. The separation between ruthenium and FAD is the smallest for site A (Figure 6). There are three very closely localized solutions (one is shown in Figure 6). The distance between Ru and nitrogen N5 of FAD of the lumichrome ring equals 21 Å and should be compared with 19 Å estimated from the electrochemical data. The fourth site (B) is separated from site A by ~10 Å, the Ru–5N(FAD) distance being 25 Å. If ruthenium were located in site B, the estimated<sup>39</sup> electron-transfer rate constant  $k_{\text{intra}}$  should be around 1 s<sup>-1</sup>, significantly lower than the experimentally obtained  $k_{\text{intra}}$  value.

Other possible localizations identified are separated from 5N(FAD) by 30 Å and more. These do not seem to play any role in bioelectrocatalysis because there should be no electron coupling between Ru and FAD in these case. Thus, the results of the electrochemical and docking simulations suggest consistent values for the separation between the Ru center and the N5 of FAD, i.e., 19 and 21 Å, respectively. Several assumptions were made regarding both the kinetic/electrochemical properties and the geometric characteristics of the ruthenium species involved. The docking simulation identifies *geometrically* favorable areas for Ru fragments within the GO globule. Potential protein donor centers for Ru<sup>II/III</sup> are neglected within this level of theory. The matching distances might be viewed as indirect evidence for long-range electron transfer involving the glucose oxidase enzyme.<sup>40–42</sup>

**Operational Stability of in Situ Generated Ruthena(II)-cycle-Glucose Oxidase Assemblies.** As mentioned above, the maximum catalytic currents in the irradiated ruthena(II)cyclo-GO–D-glucose system develop after several scans (Figure 3). This is typical of all complexes **1–4**. However, these electrocatalytically active assemblies have moderate lifetimes, and the catalytic currents diminish gradually. The speed of loss of the electrocatalytic activity depends on the complex used. The best performance was observed with complex **2** (Figure 7). The electrochemical response was first stable for 2 h but then decreased rather sharply. After 5 h, the current was ~20% of the initial value. The operational stabilities of the assemblies with complexes **1** and **3** were lower. The current starts to decrease after reaching a maximum value. It is interesting to note that the final (i.e., observed after ~5 h) electrocatalytic characteristics of all preparations were the same as or similar to those of isolated ruthena(II)cyclo-GO samples. These were obtained by treating native GO with an excess of irradiated complexes **2** and **3**, followed by fractional separation on DEAE sepharose. The **3**–GO preparation, which contained ca. five Ru residues per enzyme unit, displayed lower electrocatalytic activity than the **2**–GO sample (14 residues). It is expected that GO preparations with ruthenium artificially loaded into the protein globule should denature faster under the operating conditions used. Denaturing of enzymes by heavy metal ions is a matter of common knowledge.<sup>43</sup> In addition, GO-bound ruthenium complexes might catalyze the oxidation of amino acid residues by O<sub>2</sub> or H<sub>2</sub>O<sub>2</sub>, i.e., by oxidizing agents involved in the natural

(37) Ryabova, E. S.; Goral, V. N.; Csoregi, E.; Mattiasson, B.; Ryabov, A. D. *Angew. Chem., Int. Ed.* **1999**, *38*, 804–807.

(38) Katz, E.; Riklin, A.; Heleg-Shabtai, V.; Willner, I.; Buckmann, A. F. *Anal. Chim. Acta* **1999**, *385*, 45–58.

(39) Moser, C. C.; Keske, J. M.; Warncke, K.; Farid, R. S.; Dutton, P. L. *Nature* **1992**, *355*, 796–802.

(40) Gray, H.; Winkler, J. R. *Annu. Rev. Biochem.* **1996**, *65*, 537–561.

(41) Gray, H. B.; Winkler, J. R. *Electron Transfer Chem.* **2001**, *3*, 3–23.

(42) Dmochowski, I. J.; Dunn, A. R.; Wilker, J. J.; Crane, B. R.; Green, M. T.; Dawson, J. H.; Sligar, S. G.; Winkler, J. R.; Gray, H. B. *Methods Enzymol.* **2002**, *357*, 120–133.

(43) Ercal, N.; Gurer-Orhan, H.; Aykin-Burns, N. *Curr. Top. Med. Chem.* **2001**, *1*, 529–539.

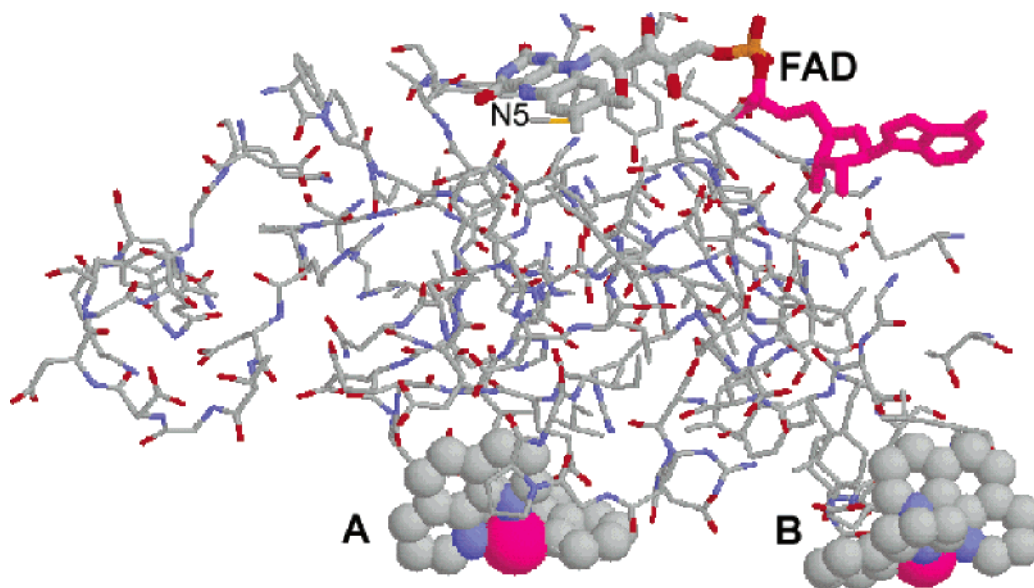


**Figure 6.** Two principle localizations of the  $[\text{Ru}(\text{o-C}_6\text{H}_4\text{-py})(\text{phen})]$  fragment (A and B) closest to the active site FAD of GO according to the docking analysis. A fragment of the entire GO structure is shown. For more detail, see text.

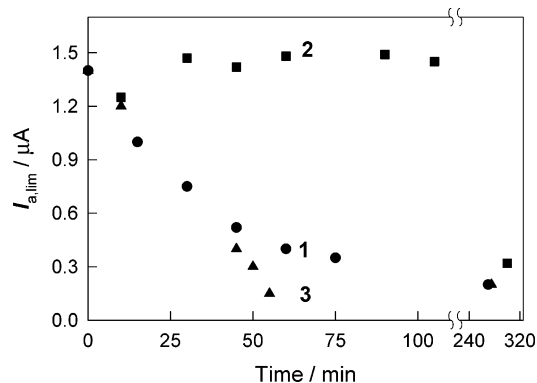


**Figure 7.** Limiting current at 0.5 V (versus SCE) as a function of time in the system ruthena(II)cyclen-GO-D-glucose for complexes (●) 1, (■) 2, and (▲) 3. Conditions as in Figure 3.

catalytic cycle of GO.<sup>3</sup> The fact that the rate of inactivation depends on the structure of the complex (Figure 7) suggests that designing the coordination sphere at  $\text{Ru}^{\text{II}}$  might increase the operational stability of Ru-GO preparations.

**Photomechanical Oscillations in the Ruthenacycle-Glucose Oxidase-D-Glucose System.** The results described above led to the idea that, if irradiation of the  $\text{Ru}^{\text{II}}$  species were carried out in water, the  $\text{Ru}^{\text{III}}$  species generated in the air might further react with GO(red) to revert to  $\text{Ru}^{\text{II}}$ . This hypothesis was actually confirmed. In addition, we found mechanically induced oscillations in the system ruthenacycle-GO-D-glucose.

When a solution of complex **2** after irradiation in MeOH was added to an aqueous buffer, a band with a maximum at 534 nm develops. This process is similar to the second, slow step of the transformation of **2** after irradiation in water (see above). The increase in the optical density at  $\sim 510$  nm is less pronounced, and therefore, the progress of the enzymatic reaction after addition of GO and D-glucose was monitored at this wavelength (Figure 8). As seen, there is a noticeable lag period after the mixing, followed by a rapid growth in absorbance. If the cell is removed from the cell compartment and vigorously shaken, the solution fades instantaneously, followed by a rapid increase in absorbance

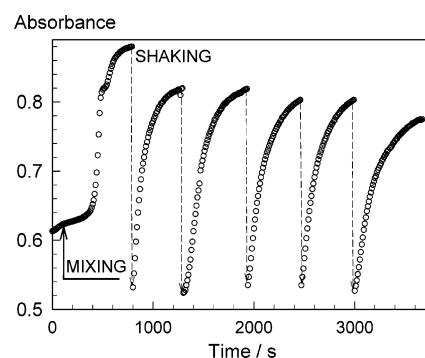
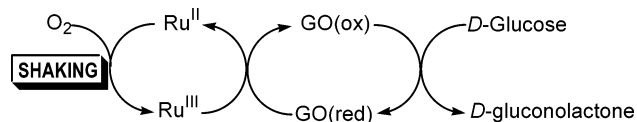


**Figure 8.** Absorbance changes at 510 nm after the mixing of irradiated complex **2** for 10 min in MeOH with GO and D-glucose in the aqueous buffer. Final conditions:  $[\mathbf{2}] = 10^{-4}$  M,  $[\text{GO}] = 10^{-7}$  M,  $[\text{glucose}] = 0.03$  M, 25 °C,  $[\text{phosphate}] = 50$  mM, pH 7.0.

### Scheme 2. Stoichiometric Mechanism Accounting for Photomechanical Oscillations in the Ruthenacycle-GO-D-Glucose System



without observable delay. The rates of absorbance increase during cycles 1 and 2 are similar. Shaking the solution after the completion of cycle 2 initiates cycle 3. The cycles could be performed many times (Figure 8). The oscillations are due to enzyme-involved redox transitions between  $\text{Ru}^{\text{II}}$  and  $\text{Ru}^{\text{III}}$  in the presence of  $\text{O}_2$  (Scheme 2). The initial increase in absorbance occurs because the enzymatic reaction between GO(red) and  $\text{Ru}^{\text{II}}$  affords GO(ox) and  $\text{Ru}^{\text{II}}$ . The  $\text{Ru}^{\text{III}} \rightarrow \text{Ru}^{\text{II}}$  half-reaction accounts for the increase in absorbance. Because  $\text{Ru}^{\text{II}}$  and GO(red) consume  $\text{O}_2$ , the reaction solution becomes short in dioxygen. Shaking increases the concentration of  $\text{O}_2$  in solution. The ruthenium(II) formed then reacts with this  $\text{O}_2$  to yield  $\text{Ru}^{\text{III}}$ , and the absorbance decreases rapidly. In the absence of  $\text{O}_2$ , the process results in accumulation of  $\text{Ru}^{\text{II}}$ . The effect of  $\text{O}_2$  is similar

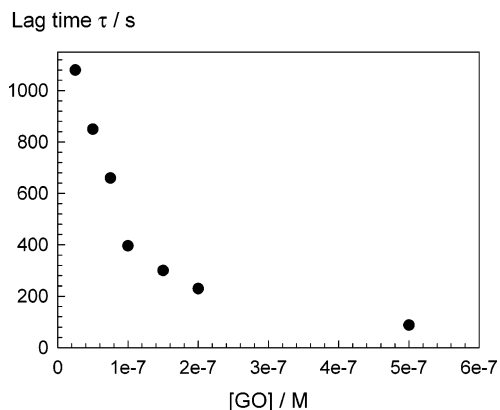


**Figure 9.** Lag period versus GO concentration observed after the mixing of all components of the oscillating system. Conditions:  $[2] = 10^{-4}$  M,  $[\text{glucose}] = 0.03$  M,  $25$  °C,  $[\text{phosphate}] = 50$  mM,  $\text{pH}$  7.0.

to the “blue bottle” experiment originally described by Campbell.<sup>44,45</sup> Dioxygen rapidly oxidizes methylene blue dye under basic conditions. The oxidized dye reacts with D-glucose to revert to methylene blue. Coichev and van Eldik reported on a related inorganic example. Metal ions  $\text{Co}^{\text{III}}$ ,  $\text{Fe}^{\text{III}}$ , and  $\text{Mn}^{\text{III}}$  oxidize sulfite into sulfate, but dioxygen converts  $\text{M}^{\text{II}}$  species into  $\text{M}^{\text{III}}$ .<sup>46–48</sup> In this case, dioxygen-induced  $\text{M}^{\text{II}} \rightarrow \text{M}^{\text{III}}$  transitions cause a color variation.

As mentioned, there is a lag period after the first mixing of all components (Figure 8) as though the system were adjusting itself to the subsequent electron transfer. The timing of the lag period does not depend on the concentration of  $\text{Ru}^{\text{II}}$  introduced. The oscillations take place at all concentrations of  $\text{Ru}^{\text{II}}$  studied. In contrast, the lag period decreases upon increasing GO concentration (Figure 9). This might indicate the role of the enzyme as a ligand in developing the catalytically active assembly. In fact, similar to the results described above (see Figure 3 and the text), the primary  $\text{Ru}^{\text{III}}$  species generated upon irradiation is insignificantly reactive toward GO, and the bioelectrocatalytic effect

develops after several scans. The explanation for this behavior is based on the postulate that the mediator should find a proper place within the enzyme interior. The same mechanistic rationale is applicable in the present case. Higher concentrations of GO accelerate the generation of biocatalytically active species.

It is interesting to note that, when the catalytically active assemble is made, no lag periods are observed after further shaking. Mechanical oscillations starting with cycle 2 are similar. The rate of the absorbance increase, which is directly proportional to the total concentration of complex **2** in the range of  $(4–10) \times 10^{-4}$  M, is constant for at least 10 oscillations. As observed electrochemically, there is a gradual decline in the catalytic activity of GO. A residual 46% activity is observed after 20 oscillations or, alternatively, 35 000 turnovers.

## CONCLUSIONS

This work describes an interesting family of cyclometalated ruthenium(II) mediators of horseradish peroxidase and glucose oxidase from *A. niger*. A new feature of these light-sensitive mediators is that they can function in aqueous medium at significantly different potentials of a working electrode. The redox potentials of the intact mediators are around +0.25 V. They are significantly lower, of  $\sim -0.25$  V versus SCE, after irradiation due photosubstitution of acetonitrile or pyridine ligands. Therefore, a driving force of electron transfer reactions involving oxidoreductases and ruthenium centers could be controllably adjusted as in the case of horseradish peroxidase. Studies of glucose oxidase in the presence of irradiated ruthenium mediators revealed that the latter interact with amino acid residues of the enzyme to give fragile electrocatalytically active assemblies within which the intramolecular electron transfer from reduced  $\text{FADH}_2$  to  $\text{Ru}^{\text{III}}$  occurs extremely rapidly at  $\sim 20$ -Å separation of the redox partners.

## ACKNOWLEDGMENT

We thank Dr. Michel Pfeffer for his stimulating interest in bioapplications of ruthenacycles and CONACyT for financial support (Project 34293-E).

Received for review August 23, 2004. Accepted November 29, 2004.

AC048743G

(44) Campbell, J. A. *J. Chem. Educ.* **1963**, *40*, 578–583.

(45) Cook, A. G.; Tolliver, R. M.; Williams, J. E. *J. Chem. Educ.* **1994**, *71*, 160–161.

(46) Coichev, N.; Reddy, K. B.; Van Eldik, R. *Atm. Environ. A: Gen. Top.* **1992**, *26A*, 2295–2300.

(47) Coichev, N.; van Eldik, R.; Franz, D. A. *J. Chem. Educ.* **1994**, *71*, 767–769.

(48) Brandt, C.; Fabian, I.; van Eldik, R. *Inorg. Chem.* **1994**, *33*, 687–701.